ACS Medicinal Chemistry Letters

Letter

Synthesis and Pharmacological Evaluation of Selective Histone Deacetylase 6 Inhibitors in Melanoma Models

Mauricio Temotheo Tavares, Sida Shen, Tessa Knox, Melissa Hadley, Zsofia Kutil, Cyril Barinka, Alejandro Villagra, and Alan P. Kozikowski

ACS Med. Chem. Lett., **Just Accepted Manuscript** • DOI: 10.1021/acsmedchemlett.7b00223 • Publication Date (Web): 05 Sep 2017

Just Accepted

ACS Publications

ACS Medicinal Chemistry Letters is published by the American Chemical Society. 1155 Sixteenth Street N.W., Washington, DC 20036

Synthesis and Pharmacological Evaluation of Selective Histone Deacetylase 6 Inhibitors in Melanoma Models

Maurício T. Tavares,[†‖] Sida Shen,[†‖] Tessa Knox,[‡] Melissa Hadley,[‡] Zsófia Kutil,[§] Cyril Bařinka,[§] Alejandro Villagra,[‡*] and Alan P. Kozikowski[#*]

[†] Department of Medicinal Chemistry and Pharmacognosy, College of Pharmacy, University of Illinois at Chicago, IL, 60612, United States.

[‡] Department of Biochemistry and Molecular Medicine, The George Washington University, Washington, DC, 20052, United States.

[§] Institute of Biotechnology, Academy of Sciences of the Czech Republic, BIOCEV, Prumyslova 595, 252 50 Vestec, Czech Republic.

[#] StarWise Therapeutics LLC. University Research Park, Inc., 510 Charmany Drive, Madison, Wisconsin, 53719, United States.

[‖]These authors contributed equally to this work.

KEYWORDS: HDAC6 inhibitors, Nexturastat A, Melanoma, Inflammatory response, Immune response

ABSTRACT: Only a handful of therapies offer significant improvement in the overall survival in cases of melanoma, a cancer whose incidence has continued to rise in the past 30 years. In our effort to identify potent and isoform-selective histone deacetylase (HDAC) inhibitors as a therapeutic approach to melanoma, a series of new HDAC 6 inhibitors based on the nexturastat A scaffold were prepared. The new analogs **4d**, **4e**, and **7b** bearing added hydrophilic substituents, so as to establish additional hydrogen bonding on the rim of the HDAC6 catalytic pocket, exhibit improved potency against HDAC6 and retain selectivity over HDAC1. Compound **4d** exhibits anti-proliferative effects on several types of melanoma and lymphoma cells. Further studies indicates that **4d** selectively increases acetylated tubulin levels *in vitro* and elicits an immune response through down-regulating cytokine IL-10. A preliminary *in vivo* efficacy study indicates that **4d** possesses improved capability to inhibit melanoma tumor growth, and that this effect is based on the regulation of inflammatory and immune responses.

Melanoma is a common type of skin cancer that is potentially lethal, and whose incidence has doubled over the past 30 years. Despite the progress made in the understanding of the cell biology, genetics, and immunology of melanoma, the outcome for patients with advanced-stage disease has remained modest with a median survival period ranging from 12 to 24 months and with an overall survival rate at 5 years of less than 20%.[1] A few advancements have recently been achieved for metastatic melanoma with mutation-based targeted therapies such as the dabrafenib and trametinib for the treatment of melanoma with $BRAF^{V600E}$ or $BRAF^{V600K}$ mutations[2], and with immune checkpoint blockade [e.g., ipilimumab (CTLA-4) and pembrolizumab (PD-1)].[3] However, primary nonresponse and acquired resistance to therapy remain challenges and require the development of novel treatment approaches.[4] One of the recent advances in cancer treatment focuses on the role of epigenetic modifiers in the regulation of immuno-modulatory pathways.[5] Among these, histone deacetylases (HDACs) are attractive targets due to the availability of several marketed, broad-spectrum inhibitors of these zinc-containing enzymes. Several pan-HDAC inhibitors (HDACis) such as vorinostat, panobinostat, and quisinostat have recently been tested in Phase I or early Phase II trials for melanoma, yet most of these show limited efficacy and tolerability as single agents (Figure 1), with hematological toxicity, fatigue, nausea, and laboratory abnormalities occurring as frequent adverse effects.[6] Significant wider concerns regarding pan-HDACis are also rising since their broad activity may cause unwanted off-target effects that may impair their tolerability in clinical use. Since "one-size-fits-all" approaches have been dominating the design of new HDACis, the relevance of targeting one specific HDAC isoform has not been well established. In our prior work, we have demonstrated that pan-HDACis possess anti-tumor activity through direct cytotoxicity and improved immune responses.[7] There is now growing interest in developing isozyme-selective HDACis that maintain beneficial effects but exhibit reduced toxicity or deleterious effects compared to broad-spectrum inhibitors.[8]

HDACs are a family of proteins responsible for catalyzing the hydrolysis of acetylated lysine residues in histones to provide free lysine residues.[9] There are 18 known mammalian HDACs, which are divided into 4 classes, based on their sequence similarity to yeast homologs: class I (HDAC1, 2, 3, and 8), class IIa (HDAC4, 5, 7, and 9), class IIb (HDAC6 and 10), class III (SIRT1-7), and class IV (HDAC11).[10-12] Among these isoforms, HDAC6 has received particular attention in the last 10 years due to its relative uniqueness within its family. Unlike

its related family members, HDAC6 contains two tandem protein deacetylase catalytic domains (CD1 and CD2), primarily within the cytosol rather than the nucleus, and has no apparent role in the post-translational modification of histone proteins, but rather is involved in regulating the acetylation status of α-tubulin, cortactin, HSP-90, HSF-1, and other non-histone proteins.[13] We previously identified a potent and highly selective HDAC6i named nexturastat A (NexA, Figure 1), which presents low micromolar anti-proliferative activity *in vitro* against a panel of human melanoma cell lines including both mutant and wild type NRAS/BRAF.[14] Further experiments demonstrated that treatment with NexA *in vivo* resulted in both impaired tumor growth and increased tumor-specific immunogenic signals, which are characteristics highly desired in anticancer therapies.[7,15]

Herein, we report further structure-activity relationship (SAR) studies in a series of compounds based on the NexA scaffold bearing a urea as cap, a benzyl linker, and a hydroxamate moiety as zinc-binding group (ZBG). Furthermore, we provide evidence that these NexA analogs, while displaying only modest anti-proliferative effects on melanoma cell lines, possess an improved capability to inhibit tumor growth in a melanoma xenograft model, and that this effect is based on the regulation of inflammatory and immune responses rather than direct cytotoxicity.

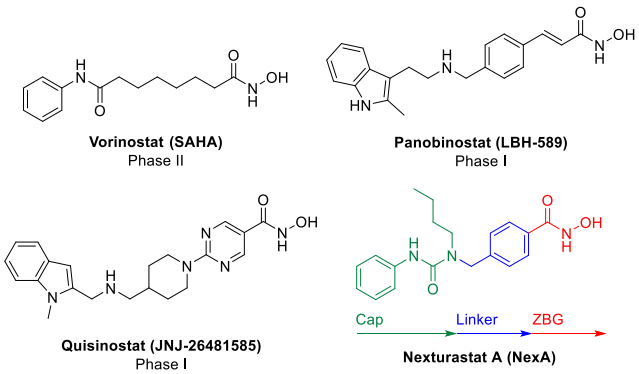

Figure 1. Structures of nexturastat A, and hydroxamate based HDACis in clinical trials for melanoma.

In general, HDACis contain three main motifs: a cap group that interacts with the surface of the enzyme, a linker group that occupies a hydrophobic channel, and a ZBG that coordinates with the zinc ion (Zn^{2+}) at the bottom of the catalytic pocket (Figure 1). Previously, we reported that a side chain, attached to the urea nitrogen proximal to the benzyl linker, plays a significant role for improving both HDAC6 selectivity and potency.[14] Thus, to explore additional modifications in the cap region, we initially designed and synthesized analogs **4a-e** with phenyl replaced by amine-substituted phenyl and by different nitrogen heterocycles, while the *n*-butyl-substituted urea motif as present in NexA was retained (Scheme 1). The synthesis of these compounds began with the two-step reductive amination of aldehyde **1** with *n*-butylamine to generate a common ester intermediate **2**. The reaction between **2** and appropriate phenyl carbamates afforded the urea derivatives **3a-e**.[14] The final products **4a-e** were obtained by reaction of these precursors with aqueous hydroxylamine under basic conditions.

To investigate the effect of the structure of the alkyl side chain attached to the proximal urea nitrogen, analogs **7a-c** bearing isobutyl, 4-hydroxybutyl, and phenethyl substituents were synthesized (Scheme 1). Methyl 4-formylbenzoate **1** underwent rapid reductive amination with the appropriate amines to provide intermediates **5a-c**, followed by reaction with phenyl isocyanate or isopropyl chloroformate to generate compounds **6a-c**. Further transformation to the hydroxamic acids **7a-c** was efficiently performed as above. To synthesize the analog **7d** bearing a phenyl linker instead of a benzyl linker (Scheme 1), methyl 4-aminobenzoate (**9**) underwent reductive alkylation to give the intermediate ester **5d**, which upon treatment with 3-nitrophenyl isocyanate afforded the urea intermediate **10**. This compound was subjected to a two-step procedure consisting of hydrogenation and reductive alkylation using zinc-modified cyanoborohydride[16] and aqueous formaldehyde to provide the ester **6d** in high yield, which gave the hydroxamate product **7d** in the usual manner.

Scheme 1. Synthesis of analogs 4a-e, 7a-d, 8, and 14a-d.[a]

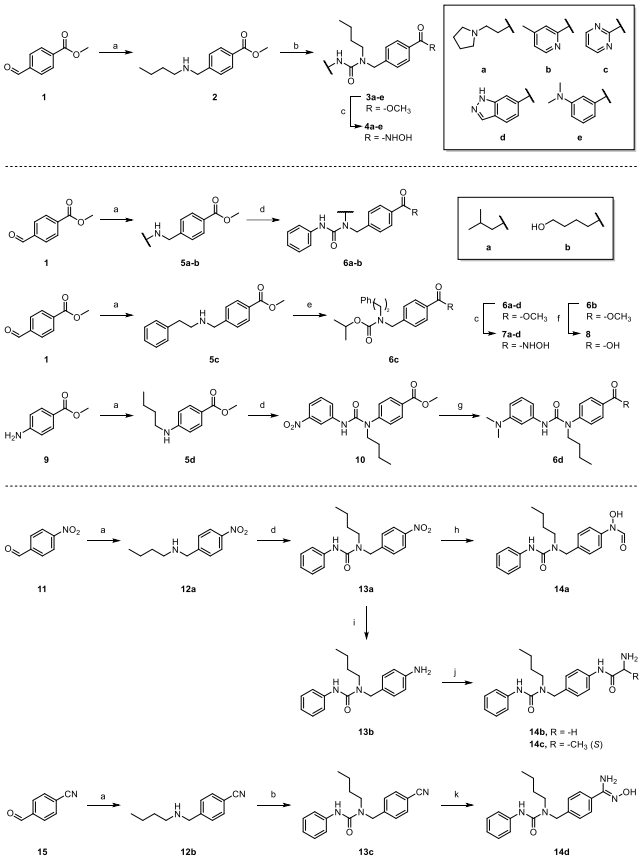

[a]Reagents and conditions: a) i. amine, EtOH, reflux, 2 h; ii. $NaBH_4$, MeOH, 0 °C-r.t., 2 h; b) *N*-substituted carbamic acid phenyl esters, TEA, THF, reflux, 2 h; c) NH_2OH (50 wt. % in H_2O), NaOH, THF/MeOH, 0 °C, 15 min. d) phenyl isocyanate or 3-nitrophenyl isocyanate, DCM, r.t., overnight; e) i-PrOCOCl, DIPEA, DCM, 0 °C-r.t., 1 h; f) 1N NaOH, THF/MeOH, r.t., overnight; g) i. H_2, 10% Pd/C, MeOH, r.t., 1 h; ii. aq. CH_2O, $NaCNBH_3$, $ZnCl_2$, MeOH, r.t., 3 h. h) i. $N_2H_4 \cdot H_2O$, 5% Pd/C, 0 °C, 1 h; ii. formic acid, EDCI, THF, 0 °C, 3 h; i) H_2, 10% Pd/C, MeOH, r.t., 1 h; j) i. Boc-glycine or Boc-*L*-alanine, HATU, DIPEA, THF, r.t., 16 h; ii. TFA, DCM, r.t., 1 h; k) NH_2OH (50 wt. % in H_2O), EtOH, 80 °C, 3 h.

To explore alternative ZBGs, the non-hydroxamate analogs **8** and **14a-d** were synthesized (Scheme 1). The carboxylic acid analog **8** was directly obtained from the ester **6b** by basic hydrolysis. To synthesize the retro-hydroxamate **14a**, 4-nitrobenzaldehyde (**11**) underwent reductive amination and then reaction with phenyl isocyanate to produce the urea intermediate **13a**. This compound was partially hydrogenated with hydrazine

catalyzed by 5% Pd/C, and the resulting arylhydroxylamine was condensed with formic acid to afford the final product **14a**. The aniline intermediate **13b** was obtained by standard catalytic hydrogenation from its nitro precursor **13a** and was acylated with Boc-glycine or Boc-*L*-alanine under HATU condition. Deprotection with TFA provided the analogs **14b-c**. To synthesize compound **14d**, 4-formylbenzonitrile (**15**) was first converted to the intermediate **13c** *via* reductive amination and reaction with phenyl isocyanate. Upon treatment with aqueous hydroxylamine under reflux, compound **13c** gave the final product **14d**.

Inhibitory activity of new analogs was initially evaluated against the HDAC1 and 6 isoforms (Table 1), and the four most potent and selective compounds were further tested against HDAC8 (Table S1). As is apparent from the data shown in Table 1, replacement of the aryl cap with a non-aromatic heterocycle as in compound **4a** led to a significant decrease in potency at both HDAC1 and HDAC6 (>14000 and 74 nM, respectively) compared to NexA, suggesting that the interaction of the aryl cap and the enzyme surface is necessary for potent binding. Additionally, the increased flexibility and rotational freedom available to **4a** would result in a greater loss of configurational entropy upon protein binding compared with a more rigid scaffold, and lead to a penalty in its potency. Heteroaromatic rings or an amine-substituted phenyl group as cap groups (compounds **4b-e**) were beneficial for maintaining excellent potency except in compound **4b**, which displayed an ~8 fold decrease in activity compared to NexA. We assume that the additional nitrogen groups present in the indazole ring of **4d** or in the dimethylaniline moiety of **4e** contribute to binding through engagement in additional hydrogen bonds with amino acids on the rim of the pocket.

Our previous SAR study on NexA has demonstrated the importance of a lipophilic alkyl chain on the proximal urea nitrogen for HDAC activity. The isobutyl analog **7a** retained both high potency at HDAC6 (IC_{50} = 12 nM) and excellent selectivity over HDAC1, suggesting a certain tolerance for bulky alkyl chains in this position. Additionally, the introduction of a hydroxyl group at the end of the *n*-butyl chain (compound **7b**) significantly improved potency against HDAC6. This finding suggests that an additional hydrogen bonding interaction may be established, thereby enhancing the interaction with the rim of the cavity. Deletion of one nitrogen and of the carbonyl group of the urea moiety together with the attachment of an electron-withdrawing group (an isopropoxycarbonyl group, compound **7c**) as a side chain in lieu of butyl resulted in decreased HDAC6 activity (IC_{50} = 53 nM). Lastly, shortening the linker from benzyl to phenyl (compound **10c**) resulted in a ~300-fold decrease in potency compared to **4e**. We further tested the inhibitory activity of **4c-e** and **7b** at HDAC8, and compounds **4d**, **4e**, and **7b** displayed more than 500 fold selectivity over this class I isoform (Table S1).

The carboxylic acid **8**, in contrast to the related hydroxamate **7b** which displayed subnanomolar potency at HDAC6, did not show any activity at concentrations up to 30 μM. We further evaluated compounds **14a-d** bearing non-hydroxamate ZBGs, which were chosen from a variety of such groups appearing in recent publications.[17–19] Only the retro-hydroxamate analog **14a** showed low-micromolar potency at HDAC6, which may provide an opportunity to further refine HDAC6is with this alternative ZBG.

Table 1. HDAC inhibitory activity of NexA analogs 4a-e, 7a-e, 8, and 14a-d.[a]

Compd.	HDAC isoform inhibitory activity (IC_{50}, nM)		Selectivity Index
	HDAC1	HDAC6	HDAC1/6
NexA[b]	3,020 ± 740	5 ± 0.06	600
4a	14,400 ± 1,500	74 ± 4	194
4b	7,540 ± 145	43 ± 4	176
4c	2,740 ± 85	6 ± 1	456
4d	721 ± 1	1.6 ± 0.2	450
4e	604 ± 17	1.7 ± 0.2	355
7a	6,130 ± 240	12 ± 0.4	511
7b	2,913 ± 929	0.87 ± 0.66	3350
7c	5,740 ± 530	53 ± 11	107
7d	>30,000	1,790 ± 60	>17
8	N.D.[c]	N.A.[d]	-
14a	>30,000	1,025 ± 253	>29
14b	N.D.[c]	N.A.[d]	-
14c	N.D.[c]	N.A.[d]	-
14d	N.D.[c]	N.A.[d]	-
SAHA	31 ± 12	2.8 ± 2.34	11

[a]IC_{50} values displayed are the mean of two experiments ± standard deviation obtained from curve fitting of a 10-point enzyme assay starting from a 30 μM concentration of each analog with 3-fold serial dilution. Values are extracted from fitting dose–response curves to the data points. [b]Reference 14. [c]Not determined. [d]No activity.

Although three-dimensional structures of many HDACs have been reported, no crystal structures of HDAC6 catalytic domains were available until last year. Compared to most HDAC isoforms, HDAC6 is unique as it contains tandem deacetylase catalytic domains (CD) designated CD1 and CD2. Two groups respectively reported the crystal structures of both catalytic domains of HDAC6 in complex with several substrates and inhibitors, which provided mechanistic insights into the catalytic mechanism, substrate specificity, and inhibitor selectivity of HDAC6.[20,21] Early studies indicated that both domains are catalytically active toward histone substrates, with only CD2 exhibiting tubulin deacetylase activity,[22,23] whereas subsequent studies suggested that only CD2 is catalytically active.[24] It was demonstrated that different point mutations in the sequence encoding CD1 do not result in compromised deacetylation activity on α-tubulin. CD2 active sites are highly conserved and feature the typical narrow hydrophobic channel formed by residues Pro464, Gly582, Phe583, Phe643, and Leu712. The Zn^{2+} ion is coordinated by Asp612, His614, and Asp705 in CD2.[20,21] Thus, we mainly focused our attention on CD2 and carried out molecular modeling studies using the available CD2-NexA complex as template (PDB entry: 5G0I).

Docking simulations were performed for the selected compounds **4d**, **7b**, and **14a**. The best-scored poses of each compound as well as the published conformation of NexA bound to CD2 are presented in Figure 2. The docking poses of compounds **4d** and **7b** revealed a binding mode quite consistent with that of NexA in which only the hydroxamate C=O group engages in coordination with Zn^{2+} and binding is further reinforced by hydrogen bonds between NH and Gly582 of the backbone; C=O and Tyr745; and OH and His573, respectively. For compound **14a**, both OH and formyl groups of the retro-hydroxamate engage in bi-chelation with Zn^{2+}, and in additional hydrogen bonds with His573 and Tyr745, respectively. The residues Phe583 and Phe643 located in the hydrophobic channel

engage in a π-stacking interaction with the benzyl linker for all three compounds, which is consistent with the π-stacking arrangement observed for NexA. One of the nitrogen atoms in the indazole ring of compound **4d** and the oxygen atom in the hydroxybutyl chain of compound **7b** engage in hydrogen bonding interactions with the carbonyl groups of Ala641 and Leu712 backbones, respectively, which could be responsible for the improved HDAC6 activity of these compounds. Additionally, an overlay of the structures of NexA and its analogs indicates that the proximal urea nitrogen plays a significant role in keeping the structural features related to the tetrahedral steric configuration of these compounds favoring the interaction (Figure S1).

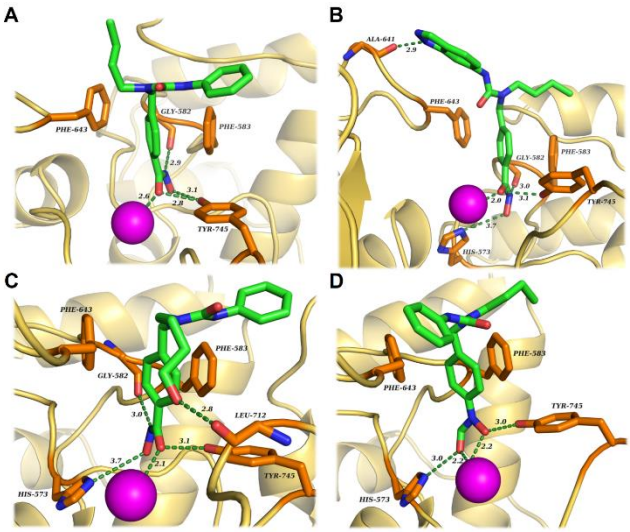

Figure 2. (A) Crystal structure of the complex of NexA (green) with HDAC6 CD2 [PBD entry: 5G0I]. (B) Binding interaction of **4d** (green) with HDAC6 CD2 (ΔG_{exp} = -10.3 kcal/mol). (C) Binding interaction of **7b** (green) with HDAC6 CD2 (ΔG_{exp} = -11.0 kcal/mol). (D) Binding interaction of **14a** (green) with HDAC6 CD2 (ΔG_{exp} = -8.9 kcal/mol).

We previously reported that NexA exhibits micromolar anti-proliferative activities against human melanoma cell lines bearing different mutations, and found that HDACis possessed anti-cancer effects both through direct cytotoxicity and improved immune responses.[7,14] To investigate the effect of our newly developed compounds in cells, MTS proliferation assays using the selected analogs **4c**-**e** were conducted in different types of melanoma and lymphoma cell lines, including the murine SM1, B16, and FcMCL cell lines which have been widely used in the *in vitro* and *in vivo* screening of HDACis and other epigenetic modifiers in syngeneic models aiming to study anti-tumor immune responses (Figure S2).[7,25] Notably, compounds **4c** and **4d** displayed consistent modest anti-proliferative effects on these cell lines at concentrations increasing from 1 μM to 15 μM, while compound **4e** displayed more obvious anti-proliferative effects in murine FcMCL lymphoma cells and murine B16 melanoma cells at lower concentrations.

Acetylated α-tubulin is an important physiological substrate for HDAC6 and is not deacetylated by other zinc-containing HDACs. In contrast, HDAC6 does not influence the acetylation status of histone 3 (H3), which is mainly deacetylated by the class I HDACs. The analysis of these two substrates indicates whether HDAC6 is selectively inhibited in the concentration range used in the anti-proliferation experiments. Thus, we further measured the selective effects of these compounds on the acetylation status of both H3 and α-tubulin in human WM795 melanoma cells with the same dose range to determine cell-based HDAC specificity. As is apparent from Figure 3B, acetylated α-tubulin levels increased dramatically upon treatment with NexA and **4c**-**e** at each concentration compared to the non-treatment conditions, although we didn't observe obvious effects in the MTS cell line assays. Moreover, the acetylation status of H3 remained unaltered or increased slightly in the presence of all HDAC6is at all tested concentrations.

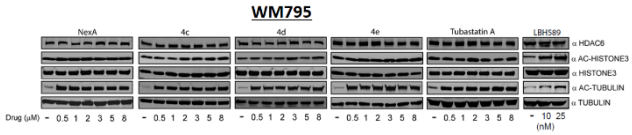

Figure 3. Western blot illustrating tubulin acetylation and histone acetylation levels in WM795 melanoma cells following 24 h treatment with increasing concentrations of NexA and analogs **4c**-**e**. The selective HDAC6 inhibitor tubastatin A and the pan-HDAC inhibitor LBH-589 were included on each blot as positive controls. Protein extracts were prepared and subjected to SDS-PAGE and immunoblotting with α-HDAC6, α-tubulin, α-acetylated tubulin, α-histone 3, and α-acetylated H3 specific antibodies. This figure is representative of three independent experiments.

Melanomas are highly immunogenic and often heavily infiltrated by various types of immune cells. In these cancers, the immune system fails to eradicate the tumor cells which is usually related to negative regulation by tumor-generated immunosuppressive cytokines, in particular interleukin-10 (IL-10).[26,27] IL-10 is produced by tumor-associated macrophages and tumor-related lymphocytes associated with early stages of tumor evolution, and its levels are elevated in serum obtained from patients with later stages of melanoma.[28] IL-10 is generally accepted as a major immunosuppressive cytokine, and its expression was reported for several types of cancers but not in adjacent non-malignant tissue of the patients.[29-31] We previously reported that the treatment of antigen-presenting cells (APCs) such as macrophages and dendritic cells with selective HDAC6is *in vitro* and *in vivo* improved T-cell activation *via* diminished production of a major immunosuppressive cytokine, IL-10. This effect was not observed in experiments performed using pan-HDACis.[32,33] Thus, our next step was to determine the effect of treatment with compound **4d** on the production of IL-10 in macrophages after stimulation with lipopolysaccharide (LPS). Interestingly, the treatment of primary peritoneal elicited macrophages (PEMs) isolated from C57BL/6 mice and murine macrophage RAW264.7 cells with 3 μM of **4d** down-regulated the production of IL-10 after 24 h treatment (Figure 4A). Outcome observed previously when using other HDAC6is.[32] Additionally, an initial metabolism assessment showed that compound **4d** was metabolically stable both in human ($t_{1/2}$ = 408 min) and mouse ($t_{1/2}$ = 239 min) liver microsomes, which is beneficial for animal studies in the next stage (Figure S3).

To this end, C57BL/6 mice bearing B16-F10-luc melanoma tumors were treated with **4d** (20 mg/kg) for 22 days, resulting in 100% survival rates and significant reduction of tumor volumes compared to the vehicle group (40% survival) (Figure 4B and 4C). Therefore, the experiment continued with the same dosage until the last animal in the control group died (or the tumor reached 2500 mm^3). Moreover, an improved ability of **4d** to inhibit tumor growth was observed in comparison with another selective HDAC6i, tubastatin A (Figure 4C). In contrast, no significant effect on the growth of B16-F10 melanoma tumors was observed in immunodeficient (SCID) mice after treatment with compound **4d** for 20 days (Figure 4D). This result indicates that the mechanism for the compound's action is the regulation of inflammatory and immune responses. These *in*

vivo data have been partly disclosed in our previous publication.[7]

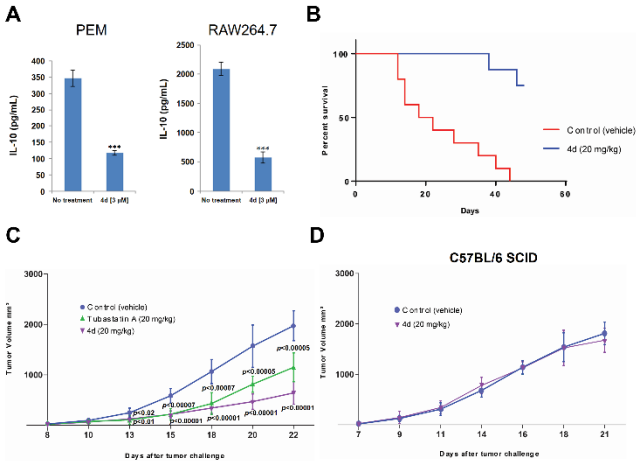

Figure 4. (A) Murine peritoneal elicited macrophages (PEM) (left) and murine RAW264.7 macrophage cells (right) were treated with LPS (1 μg/mL) or LPS plus 3 μM of compound **4d** for 24 hours. Supernatants were then collected, and the production of IL-10 was determined by ELISA. ***p<0.001 as compared to the untreated cells. (B-D) *In vivo* tumor growth of C57BL/6 mice injected subcutaneously with B16-F10-luc WT cells. Mice were treated by intraperitoneal injection daily with the compound **4d** (20 mg/kg). Survival (B) and tumor growth (C) were monitored throughout the experiment. (D) *In vivo* tumor growth of B16-F10 WT melanoma cells in immunodeficient SCID mice treated with **4d** compared with control vehicle treatment.

In conclusion, fourteen new NexA derivatives with different caps, linkers, and ZBGs were designed, synthesized, and initially evaluated in class I and class IIb HDACs. Several hydroxamate-based analogs exhibited improved potency against HDAC6 compared to NexA while maintaining excellent selectivity over HDAC1 and 8. The selectivity of **4c**, **4d**, and **4e** was further verified in melanoma cells in terms of increasing levels of acetylated tubulin rather than levels of acetylated histone. Moreover, the analog **4d** exhibited modest *in vitro* anti-proliferative effects in different types of melanoma cells and human lymphoma cells, but significantly down-regulated the production of the immunosuppressive cytokine IL-10 in macrophages. The *in vivo* efficacy study of the metabolically stable HDAC6 inhibitor **4d** demonstrated improved capability to inhibit tumor growth in melanoma models through the regulation of inflammatory and immune responses. While Ames activity does not typically constitute a go/no go decision in advancing cancer drugs (the hydroxamate-based HDAC inhibitors vorinostat and panobinostat are Ames active), a lack of Ames activity would be of benefit in terms of avoiding mutagenic events that may lead to the generation of secondary tumors.[34] As such, the lead compound **4d** will be further evaluated in mutagenicity assays, as well as profiled in other standard ADMET assays. Moreover, we plan follow-up mechanistic studies to investigate HDAC6i-induced regulation of other immunosuppressive cytokines in melanoma cancer models.

ASSOCIATED CONTENT

Supporting Information

Supplementary figures, details of the synthetic chemistry, *in silico* studies, and biological assays is available free of charge on the ACS Publications website (PDF).

AUTHOR INFORMATION

Corresponding Author

A.V.: e-mail: avillagra@email.gwu.edu. Phone: (+1) 202 994 9547;

A.P.K.: e-mail: AKozikowski@starwisetrx.com. Phone: (+1) 312 996 7577.

Funding Sources

This work was supported by the NIH (NS079183, to A.P.K.; CA184612 and MRF CDA grant award, to A.V.), and by the CAS (RVO: 86652036), project BIOCEV (CZ.1.05/1.1.00/02.0109) from the ERDF, and CSF to C.B. (15-19640S).

Notes

The authors declare no competing financial interests.

ACKNOWLEDGMENT

The authors gratefully acknowledge Dr. Werner Tueckmantel for reviewing the article and providing comments.

ABBREVIATIONS

CTLA-4, cytotoxic T lymphocyte associated protein 4; PD-1, programmed cell death protein 1; HDAC, histone deacetylase; HDACi, histone deacetylase inhibitor; SIRT, sirtuin; CD, catalytic domain; HSP-90, heat shock protein 90; HSF-1, heat shock factor 1; NexA, Nexturastat A; NRAS, neuroblastoma RAS gene; BRAF, B-Raf proto-oncogene; SAR, structure-activity relationship; ZBG, zinc-binding group; DIPEA, *N*,*N*-diisopropylethylamine; HATU, 1-[bis(dimethylamino)methylene]-1*H*-1,2,3-triazolo[4,5-*b*]pyridinium 3-oxide hexafluorophosphate; TFA, trifluoroacetic acid; EDCI, 1-ethyl-3-(3-dimethylaminopropyl)carbodiimide; PDB, Protein Data Bank; MTS, 3-(4,5-dimethylthiazol-2-yl)-5-(3-carboxymethoxyphenyl)-2-(4-sulfophenyl)-2H-tetrazolium; H3, histone 3; APC, antigen-presenting cell; LPS, lipopolysaccharide; PEM, peritoneal elicited macrophage; IL-10, interleukin 10; ELISA, enzyme-linked immunosorbent assay; SCID, severe combined immunodeficiency.

REFERENCES

(1) Lens, M. B.; Dawes, M. Global perspectives of contemporary epidemiological trends of cutaneous malignant melanoma. *Br. J. Dermatol.* **2004**, *150*, 179–185.

(2) https://www.cancer.gov/about-cancer/treatment/drugs/fda-dabrafenib (accessed July 2017) and https://www.cancer.gov/about-cancer/treatment/drugs/fda-trametinib (accessed July 2017).

(3) Postow, M. A.; Callahan M. K.; Wolchok, J. D. Immune Checkpoint Blockade in Cancer Therapy. *J. Clin. Oncol.* **2015**, *33*, 1974–1982.

(4) O'Donnell, J. S.; Smyth, M. J.; Teng, M. W. L. Acquired Resistance to Anti-PD1 Therapy: Checkmate to Checkpoint Blockade? *Genome Med.* **2016**, *8*, 111.

(5) Liu, J.; Gu, J.; Feng, Z.; Yang, Y.; Zhu, N.; Lu, W.; Qi, F. Both HDAC5 and HDAC6 Are Required for the Proliferation and Metastasis of Melanoma Cells. *J. Transl. Med.* **2016**, *14*, 7.

(6) Hornig, E.; Heppt, M. V.; Graf, S. A.; Ruzicka, T.; Berking, C. Inhibition of histone deacetylases in melanoma - a perspective from bench to bedside. *Exp. Dermatol.* **2016**, *25*, 831–838.

(7) Woan, K. V.; Lienlaf, M.; Perez-Villaroel, P.; Lee, C.; Cheng, F.; Knox, T.; Woods, D. M.; Barrios, K.; Powers, J.; Sahakian, E.; Wang, H. W.; Canales, J.; Marante, D.; Smalley, K. S. M.; Bergman, J.; Seto, E.; Kozikowski, A.; Pinilla-Ibarz, J.; Sarnaik, A.; Celis, E.; Weber, J.; Sotomayor, E. M.; Villagra, A. Targeting Histone Deacetylase 6 Mediates a Dual Anti-Melanoma Effect: Enhanced Antitumor Immunity and Impaired Cell Proliferation. *Mol. Oncol.* **2015**, *9*, 1447–1457.

(8) Roche, J.; Bertrand, P. Inside HDACs with More Selective HDAC Inhibitors. *Eur. J. Med. Chem.* **2016**, *121*, 451–483.

(9) Xu, W. S.; Parmigiani, R. B.; Marks, P. Histone Deacetylase Inhibitors: Molecular Mechanisms of Action. *Oncogene* **2007**, *26*, 5541–5552.

(10) Walkinshaw, D. R.; Tahmasebi, S.; Bertos, N. R.; Yang, X. J. Histone Deacetylases as Transducers and Targets of Nuclear Signaling. *J. Cell. Biochem.* **2008**, *104*, 1541–1552.

(11) Lahm, A.; Paolini, C.; Pallaoro, M.; Nardi, M. C.; Jones, P.; Neddermann, P.; Sambucini, S.; Bottomley, M. J.; Lo Surdo, P.; Carfí, A.; Koch, U.; De Francesco, R.; Steinkühler, C.; Gallinari, P. Unraveling the Hidden Catalytic Activity of Vertebrate Class IIa Histone Deacetylases. *Proc. Natl. Acad. Sci. U. S. A.* **2007**, *104*, 17335–17340.

(12) Haberland, M.; Montgomery, R. L.; Olson, E. N. The Many Roles of Histone Deacetylases in Development and Physiology: Implications for Disease and Therapy. *Nat. Rev. Genet.* **2009**, *10*, 32–42.

(13) Imai, Y.; Maru, Y.; Tanaka, J. Action mechanisms of histone deacetylase inhibitors in the treatment of hematological malignancies. *Cancer Sci.* **2016**, *107*, 1543–1549.

(14) Bergman, J. A.; Woan, K.; Perez-Villarroel, P.; Villagra, A.; Sotomayor, E. M.; Kozikowski, A. P. Selective Histone Deacetylase 6 Inhibitors Bearing Substituted Urea Linkers Inhibit Melanoma Cell Growth. *J. Med. Chem.* **2012**, *55*, 9891–9899.

(15) Lienlaf, M.; Perez-Villarroel, P.; Knox, T.; Pabon, M.; Sahakian, E.; Powers, J.; Woan, K. V.; Lee, C.; Cheng, F.; Deng, S.; Smalley, K. S. M.; Montecino, M.; Kozikowski, A.; Pinilla-Ibarz, J.; Sarnaik, A.; Seto, E.; Weber, J.; Sotomayor, E. M.; Villagra, A. Essential Role of HDAC6 in the Regulation of PD-L1 in Melanoma. *Mol. Oncol.* **2016**, *10*, 735–750.

(16) Kim, S.; Oh, C. H.; Ko, J. S.; Ahn, K. H.; Kim, Y. J. Zinc-Modified Cyanoborohydride as a Selective Reducing Agent. *J. Org. Chem.* **1985**, *50*, 1927–1932.

(17) Wu, T. Y. H.; Hassig, C.; Wu, Y.; Ding, S.; Schultz, P. G. Design, Synthesis, and Activity of HDAC Inhibitors with a N-Formyl Hydroxylamine Head Group. *Bioorg. Med. Chem. Lett.* **2004**, *14*, 449–453.

(18) Jiao, P.; Jin, P.; Li, C.; Cui, L.; Dong, L.; Pan, B.; Song, W.; Ma, L.; Dong, J.; Song, L.; Jin, X.; Li, F.; Wan, M.; Lv, Z.; Geng, Q. Design, Synthesis and in Vitro Evaluation of Amidoximes as Histone Deacetylase Inhibitors for Cancer Therapy. *Bioorg. Med. Chem. Lett.* **2016**, *26*, 4679–4683.

(19) Nishino, N.; Yoshikawa, D.; Watanabe, L. A.; Kato, T.; Jose, B.; Komatsu, Y.; Sumida, Y.; Yoshida, M. Synthesis and Histone Deacetylase Inhibitory Activity of Cyclic Tetrapeptides Containing a Retrohydroxamate as Zinc Ligand. *Bioorg. Med. Chem. Lett.* **2004**, *14*, 2427–2431.

(20) Hai, Y.; Christianson, D. W. Histone Deacetylase 6 Structure and Molecular Basis of Catalysis and Inhibition. *Nat. Chem. Biol.* **2016**, *12*, 1–21.

(21) Miyake, Y.; Keusch, J. J.; Wang, L.; Saito, M.; Hess, D.; Wang, X.; Melancon, B. J.; Helquist, P.; Gut, H.; Matthias, P. Structural Insights into HDAC6 Tubulin Deacetylation and Its Selective Inhibition. *Nat. Chem. Biol.* **2016**, *12*, 748–754.

(22) Kawaguchi, Y.; Kovacs, J. J.; McLaurin, A.; Vance, J. M.; Ito, A.; Yao, T. P. The Deacetylase HDAC6 Regulates Aggresome Formation and Cell Viability in Response to Misfolded Protein Stress. *Cell* **2003**, *115*, 727–738.

(23) Grozinger, C. M.; Hassig, C. A; Schreiber, S. L. Three Proteins Define a Class of Human Histone Deacetylases Related to Yeast Hda1p. *Proc. Natl. Acad. Sci. U. S. A.* **1999**, *96*, 4868–4873.

(24) Haggarty, S. J.; Koeller, K. M.; Wong, J. C.; Grozinger, C. M.; Schreiber, S. L. Domain-Selective Small-Molecule Inhibitor of Histone Deacetylase 6 (HDAC6)-Mediated Tubulin Deacetylation. *Proc. Natl. Acad. Sci.* **2003**, *100*, 4389–4394.

(25) Cheng, F.; Wang, H.; Horna, P.; Wang, Z.; Shah, B.; Sahakian, E.; Woan, K. V; Villagra, A.; Pinilla-ibarz, J.; Sebti, S.; Smith, M.; Tao, J.; Sotomayor, E. M. Stat3 Inhibition Augments the Immunogenicity of B-Cell Lymphoma Cells, Leading to Effective Antitumor Immunity. *Cancer Res.* **2012**, *72*, 4440–4448.

(26) Hussein, M. R. Tumour-infiltrating lymphocytes and melanoma tumorigenesis: an insight. *Br. J. Dermatol.* **2005**, *153*, 18–21.

(27) Grütz, G. New insights into the molecular mechanism of interleukin-10-mediated immunosuppression. *J. Leukoc. Biol.* **2005**, *77*, 3–15.

(28) Itakura, E.; Huang, R. R.; Wen, D. R.; Paul, E.; Wünsch, P. H.; Cochran, A. J. IL-10 expression by primary tumor cells correlates with melanoma progression from radial to vertical growth phase and development of metastatic competence. *Mod. Pathol.* **2011**, *24*, 801–809.

(29) Kim, J.; Modlin, R. L.; Moy, R. L.; Dubinett, S. M.; McHugh, T.; Nickoloff, B. J.; Uyemura, K. IL-10 production in cutaneous basal and squamous cell carcinomas. A mechanism for evading the local T cell immune response. *J. Immunol.* **1995**, *155*, 2240–2247.

(30) Leivonen, S. K.; Kähäri, V. M. Transforming growth factor-beta signaling in cancer invasion and metastasis. *Int. J. Cancer*. **2007**, *121*, 2119–2124.

(31) Krüger-Krasagakes, S.; Krasagakis, K.; Garbe, C.; Schmitt, E.; Hüls, C.; Blankenstein, T.; Diamantstein, T. Expression of interleukin 10 in human melanoma. *Br. J. Cancer*. **1994**, *70*, 1182–1185.

(32) Cheng, F.; Lienlaf, M.; Wang, H. W.; Perez-Villarroel, P.; Lee, C.; Woan, K.; Rock-Klotz, J.; Sahakian, E.; Woods, D.; Pinilla-Ibarz, J.; Kalin, J.; Tao, J.; Hancock, W.; Kozikowski, A. P.; Seto, E.; Villagra, A.; Sotomayor, E. M. A Novel Role for Histone Deacetylase 6 in the Regulation of the Tolerogenic STAT3/IL-10 Pathway in APCs. *J. Immunol.* **2014**. *193*, 2850–2862.

(33) Cheng, F.; Lienlaf, M.; Perez-Villarroel, P.; Wang, H. W.; Lee, C.; Woan, K.; Woods, D.; Knox, T.; Bergman, J.; Pinilla-Ibarz, J.; Kozikowski, A.; Seto, E.; Sotomayor, E. M.; Villagra, A. Divergent roles of histone deacetylase 6 (HDAC6) and histone deacetylase 11 (HDAC11) on the transcriptional regulation of IL10 in antigen presenting cells. *Mol. Immunol*. **2014**, *60*, 44–53.

(34) Shen, S.; Kozikowski, A. P. Why Hydroxamates May Not Be the Best Histone Deacetylase Inhibitors - What Some May Have Forgotten or Would Rather Forget? *ChemMedChem* **2016**, *11*, 15–21.

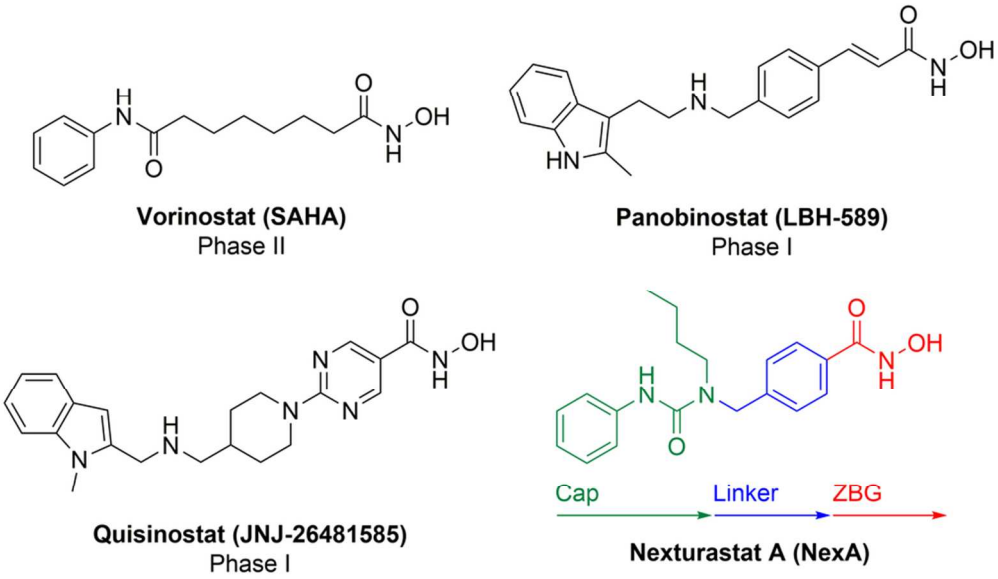

Figure 1. Structures of nexturastat A, and hydroxamate based HDACis in clinical trials for melanoma.

85x50mm (300 x 300 DPI)

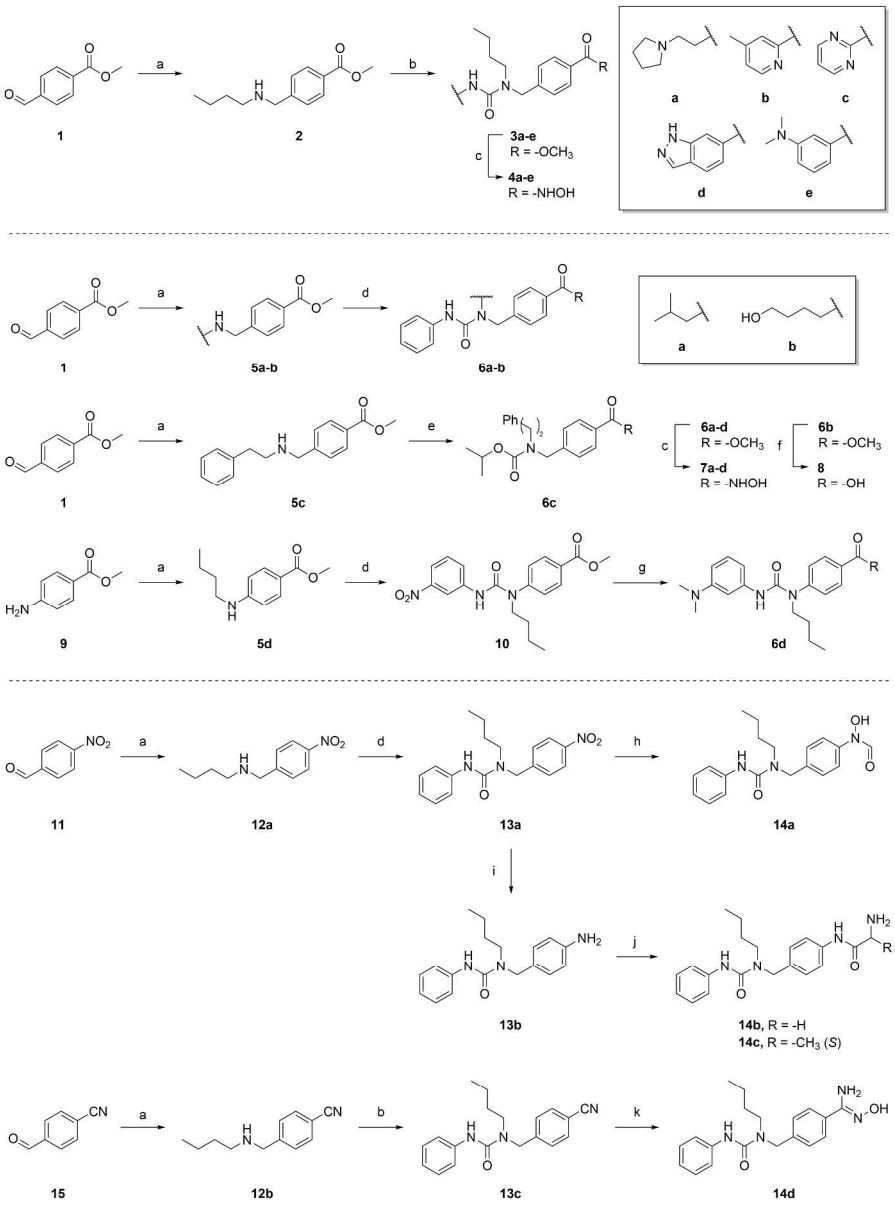

Scheme 1. Synthesis of analogs 4a-e, 7a-d, 8, and 14a-d.[a]

325x437mm (300 x 300 DPI)

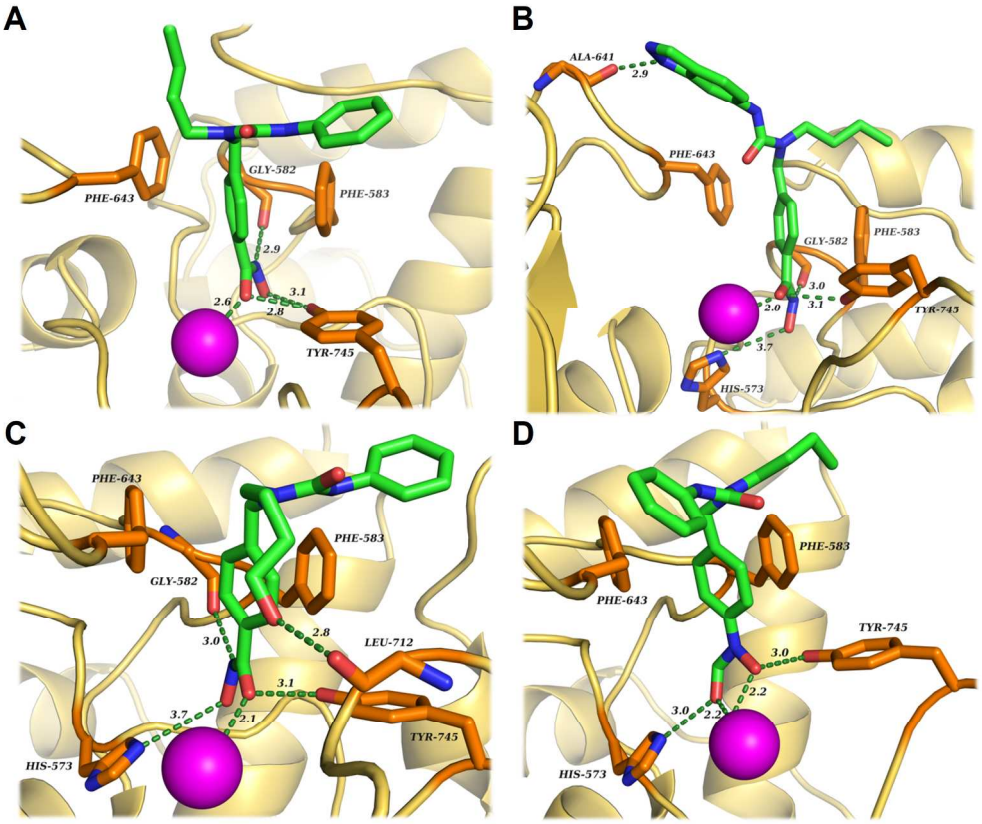

Figure 2. (A) Crystal structure of the complex of NexA (green) with HDAC6 CD2 [PBD entry: 5G0I]. (B) Binding interaction of **4d** (green) with HDAC6 CD2 (ΔG_{exp} = -10.3 kcal/mol). (C) Binding interac-tion of **7b** (green) with HDAC6 CD2 (ΔG_{exp} = -11.0 kcal/mol). (D) Binding interaction of **14a** (green) with HDAC6 CD2 (ΔG_{exp} = -8.9 kcal/mol).

659x545mm (96 x 96 DPI)

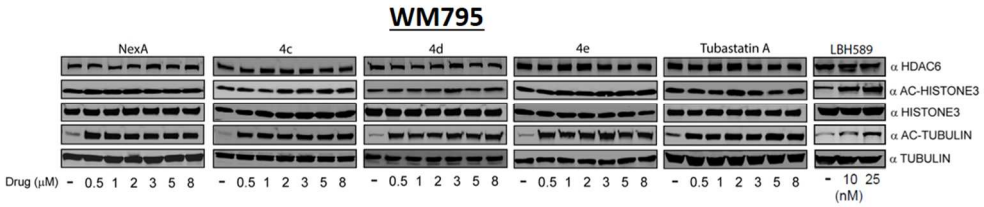

Figure 3. Western blot illustrating tubulin acetylation and histone acetylation levels in WM795 melanoma cells following 24 h treatment with increasing concentrations of NexA and analogs **4c-e**. The selective HDAC6 inhibitor tubastatin A and the pan-HDAC inhibitor LBH-589 were included on each blot as positive controls. Protein extracts were prepared and subjected to SDS-PAGE and immunoblotting with α-HDAC6, α-tubulin, α-acetylated tubulin, α-histone 3, and α-acetylated H3 specific antibodies. This figure is representative of three independent experiments.

339x70mm (96 x 96 DPI)

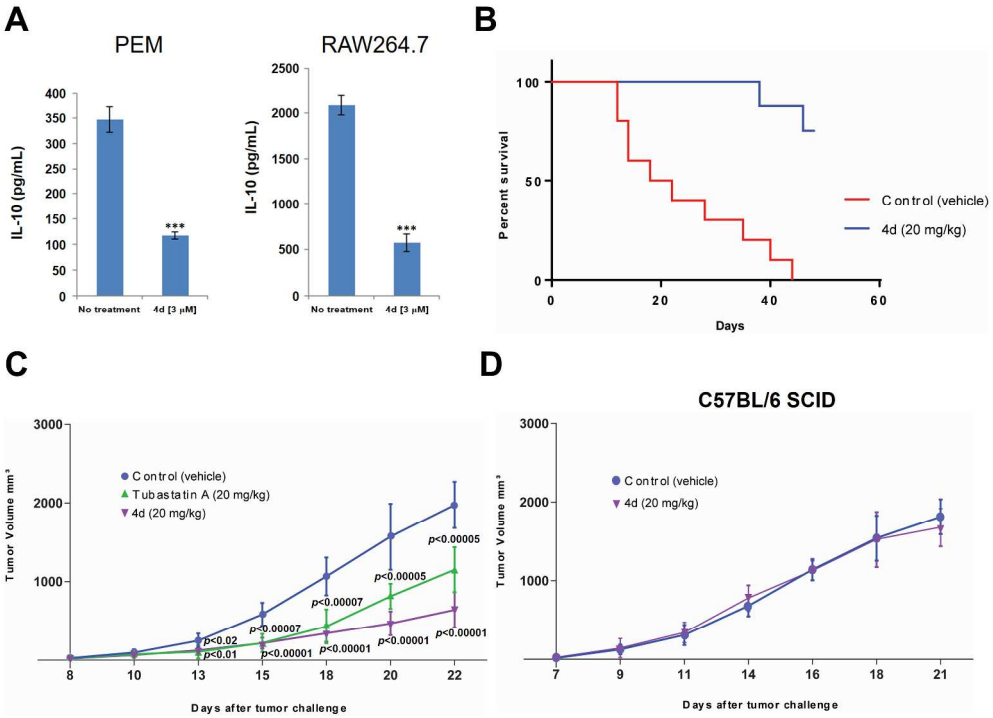

Figure 4. (A) Murine peritoneal elicited macrophages (PEM) (left) and murine RAW264.7 macrophage cells (right) were treated with LPS (1 μg/mL) or LPS plus 3 μM of compound **4d** for 24 hours. Supernatants were then collected, and the production of IL-10 was determined by ELISA. ***p<0.001 as compared to the untreated cells. (B-D) *In vivo* tumor growth of C57BL/6 mice injected subcutaneously with B16-F10-luc WT cells. Mice were treated by intraperitoneal injection daily with the compound **4d** (20 mg/kg). Survival (B) and tumor growth (C) were monitored throughout the experiment. (D) *In vivo* tumor growth of B16-F10 WT melanoma cells in immunodeficient SCID mice treated with **4d** compared with control vehicle treatment.

919x679mm (96 x 96 DPI)

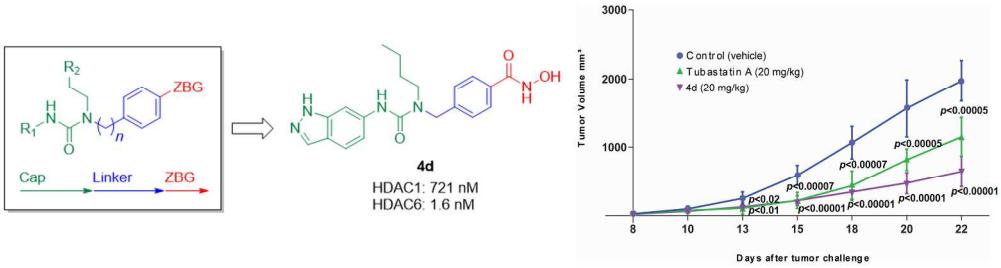

710x190mm (96 x 96 DPI)